AIP | Applied Physics Letters

Formation of antiphase domains in NiFe 2 O 4 thin films deposited on different substrates

R. Datta, S. Kanuri, S. V. Karthik, D. Mazumdar, J. X. Ma, and A. Gupta

Citation: Applied Physics Letters **97**, 071907 (2010); doi: 10.1063/1.3481365
View online: http://dx.doi.org/10.1063/1.3481365
View Table of Contents: http://scitation.aip.org/content/aip/journal/apl/97/7?ver=pdfcov
Published by the AIP Publishing

Formation of antiphase domains in $NiFe_2O_4$ thin films deposited on different substrates

R. Datta,[1,a)] S. Kanuri,[1] S. V. Karthik,[2] D. Mazumdar,[2] J. X. Ma,[2] and A. Gupta[2]
[1]*International Centre for Materials Science, Jawaharlal Nehru Centre for Advanced Scientific Research, Bangalore 560064, India*
[2]*Centre for Materials for Information Technology, 205 Bevill Building, P.O. Box 870209, University of Alabama, Tuscaloosa, Alabama 35487, USA*

(Received 16 July 2010; accepted 29 July 2010; published online 19 August 2010)

Thin films of $NiFe_2O_4$ have been deposited on various substrates using pulsed laser deposition and the defect structures investigated by transmission electron microscopy. Owing to the simultaneous nucleation of cation-disordered sites during the nonequilibrium growth, the $NiFe_2O_4$ films exhibit antiphase domains of ~20 nm, irrespective of the substrate symmetry. For growth on isostructural spinel substrates, the density of antiphase appears to decrease with decreasing lattice mismatch. Aberration corrected high resolution transmission electron microscopy reveals that the interchange of equivalent tetrahedral cation positions in the host oxygen sublattice as one of the possible mechanisms leading to the formation of antiphase domains. © *2010 American Institute of Physics*. [doi:10.1063/1.3481365]

The growth of high quality single crystalline $NiFe_2O_4$ (NFO) thin films has attracted considerable research attention recently as a candidate for microwave integrated devices,[1] magnetoelectric coupling heterostructures,[2–4] and active barrier material for emerging class of spintronic devices known as spin filters.[5–7] This is possible due to its high Curie temperature, large exchange splitting, and potentially large tunnel magnetoresistance effect. NFO is a ferrimagnetic material and its inverse spinel structure possesses many degrees of freedom for the cation arrangement under nonequilibrium condition typical of thin film growth. This offers the opportunity to tailor the properties, e.g., forming both conducting and insulating phases by controlling the growth conditions.[8] This is extremely useful for spintronic applications.[9] Moreover, transitions metal cations can acquire different oxidation states in the lattice. Controlled heteroepitaxial growth of NFO film is essential for efficient device applications. Also the relationship between atomic structure and magnetic properties of NFO films grown heteroepitaxially on various substrates needs to be understood.

The quality of NFO films grown heteroepitaxially are far from ideal compared to bulk material. Redistribution of cations toward normal spinel structure in the oxygen sub-lattice and the presence of antiphase boundaries have been accounted to be partly responsible for this behavior.[8] Recently, a low temperature growth scheme has been developed for NFO and CFO ($CoFe_2O_4$) films with improved crystal quality and magnetic property.[10] Understanding the formation of antiphase domains in NFO is important in order to improve the thin film materials performance.

Reports on the formation of antiphase domain boundary (APB) in NFO are scarce and many issues related to the heteroepitaxial growth of NFO remain unresolved. Luysberg *et al.* reported the formation of antiphase in Fe_3O_4 grown on both MgO and $MgAl_2O_4$ (MAO) substrates.[11] MgO has a rocksalt structure whereas MAO has normal spinel structure. Observation of APBs in MgO (lattice mismatch 0.33%, $Fm\bar{3}m$) and MAO (lattice mismatch 3.4%, $Fd3m$) was attributed to the presence of equivalent nucleation sites on MgO substrate (higher symmetry than NFO) and formation of misfit partial dislocations, respectively. Formation of APBs is associated with reduction in saturation magnetization in thin films due to antiferromagnetic coupling between the two antiphase domain regions. Rigato *et al.* reported magnetic properties of NFO thin films ($3\ \text{nm} \leq t \leq 32\ \text{nm}$) on both (001) $SrTiO_3$ (STO) and $MgAl_2O_4$ (MAO) substrates.[12] Ultra thin films of NFO (<20 nm for MAO and <13 nm for STO) displayed saturation magnetization values substantially higher ($M_s = 771\ \text{emu/cm}^3$ for 2.6 nm NFO film on STO and $M_s = 630\ \text{emu/cm}^3$ for 5 nm NFO film on MAO) than bulk, whereas for thick films the magnetization was observed to be low. The reduced magnetization in thicker film was attributed either to the formation of APB or cation (Ti atoms from STO to NFO) inter-diffusion between film and substrate. No concrete evidence of APBs was reported in the case of ultrathin films.

Here we report the formation and density of antiphase domains in relaxed NFO thin film grown on various substrates and the nature of antiphase boundary by electron diffraction contrast and aberration corrected phase contrast high resolution transmission electron microscopy (HRTEM). Electron diffraction contrast both in TEM cross section and plan view (PV) geometry confirms the formation of APB and HRTEM provides direct evidence on changes in the tetrahedral cation positions and its relation with APB.

NFO films on various substrates were grown by pulsed laser deposition (PLD) technique at two different temperatures, 400 and 550 °C. The deposition conditions were identical for all films: laser conditions of about $1.5\ \text{J/cm}^2$ and a high repetition rate of 10 Hz, with background oxygen pressure of 10 mTorr mixed with 10%–15% of ozone. The film growth was monitored *in situ* using reflection high energy electron diffraction. After growth, the samples were cooled down to room temperature under an ozone/oxygen pressure of 100 mTorr. Prior to deposition, the substrates were an-

a)Author to whom correspondence should be addressed. Electronic mail: ranjan@jncasr.ac.in.

TABLE I. Various substrate and qualitative comparison between lattice parameter mismatch and density of antiphase boundaries.

Substrate	Crystal structure	Lattice parameters (Å)	Dark contrast area (corresponding to APB domains)
NFO ($NiFe_2O_4$)	Inverse spinel	8.339	···
STO ($SrTiO_3$)	Perovskite	3.905	Very large
MgO (MgO)	Rock salt	4.212	Very large (<STO)
MAO ($MgAl_2O_4$)	Spinel	8.083	Medium (>CTO, <MgO<STO)
MGO ($MgGa_2O_4$)	Spinel	8.286	Small (<MAO<CTO<MgO<STO)
CGO ($CoGa_2O_4$)	Spinel	8.325	Small (<MAO<CTO<MgO<STO)
CTO (Co_2TiO_4)	Spinel	8.434	Medium (<MAO<MgO<STO)

nealed between 1300–1400 °C in air for 6 h to obtain an atomically-flat step and terrace profile. Thicknesses of the films were in the range of 200–230 nm, with the films grown at the higher temperature (550 °C) being more strain relaxed compared to those grown at lower temperature (400 °C).[10]

Table I lists NFO (lattice parameter ~8.34 Å) films grown on various substrates, crystal structure and lattice mismatch. $CoGa_2O_4$ (CGO, lattice parameter ~8.325 Å) and $MgGa_2O_4$ (MGO, lattice parameter ~8.286 Å) substrates have close lattice matching and isostructural among various substrates used for the growth. TEM thin foils were prepared by first mechanical polishing and then Ar ion milling to perforation in order to achieve wide thin electron transparent areas for both cross sectional and PV geometry. HRTEM imaging was performed in a double aberration corrected FEI TITAN^{3TM} 80–300 kV TEM with a negative spherical aberration coefficient of $C_s \sim -30$ μm and a positive defocus value of $\Delta f \sim +8$ nm. This is now commonly known as bright atom contrast imaging condition where atoms appear bright in a dark background.[13]

NFO thin films on various substrates have been observed in cross sectional TEM geometry to study the presence and density of antiphase domain boundary. Antiphase in our NFO film appears with dark diffused contrast under bright field (BF) imaging condition. Figures 1(a) and 1(b) show dark diffuse contrast corresponding to APB in NFO grown on STO (perovskite) and MAO (spinel) substrates, respectively. They seem to originate from the film substrate interface. One can also notice threading dislocations in NFO film on MAO. We have examined from TEM cross section specimens whether there is any relationship between lattice mismatch and density of dark areas. Our findings are listed in Table I for NFO films grown at 400 °C. Qualitatively, APB density is compared between various substrates from images taken under identical two beam diffraction condition (with diffracting vector g=⟨110⟩). Density of antiphase is observed to increase with increasing lattice parameter mismatch for growth on isostructural spinel substrates. For MgO (rock salt) we have noticed very high APB density although lattice parameter mismatch is only 0.33%. This may be because of higher symmetry structure of MgO-crystal with approximately half the lattice parameter as compared to NFO. The saturation magnetizations of our NFO films were determined to be 200 emu/cm^3 (on STO) and 300 emu/cm^3 (on MAO), respectively.[10] The higher population of APBs on STO substrate correlates well with the lower magnetization of NFO.

For the closely lattice matched substrates of CGO and MGO (spinel), density of APBs is smaller. Figures 2(a) and 2(b) display TEM BF images of NFO thin film grown on CGO and MGO substrates, respectively. Although APB density is less on the closely lattice matched substrates, there are other defect contrasts appearing as horizontal and vertical fringes. Diffraction pattern (DP) from NFO grown on these two substrates reveal extra spots resembling cation ordering/charge ordering [inset Figs. 2(a) and 2(b), individual diffraction pattern is placed in respective film/substrate area]. Exact cause of these extra spots need to be evaluated in details to understand their origin. In some regions fringe contrast appear to originate from the substrate, and the substrate quality may play a role in the formation of these fringe contrasts. While the STO, MgO and MAO substrates were purchased commercially, the other three (MGO, CGO, CTO) were specially grown in the laboratory of Professor A. Balbashov of the Moscow Power Engineering Institute. The crystal growth parameter not being optimized, the CGO and MGO substrates have significantly higher concentration of defects (i.e., fringe contrast seems to be originating from substrate) than the commercial substrates. For other NFO films the diffraction patterns (DPs) are single crystalline. PV TEM images from NFO/CTO, NFO/MAO, NFO/STO, and NFO/CGO show similar dark diffused contrast [Figs. 3(a)–3(d)].

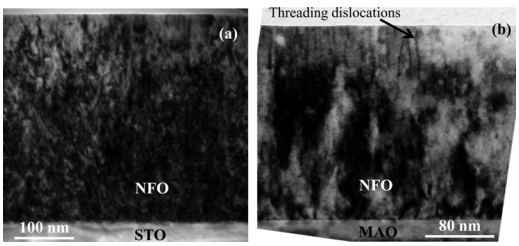

FIG. 1. TEM x-section diffraction contrast image from NFO grown on (a) STO and (b) MAO substrate. The density of APB is higher on STO compared to MAO.

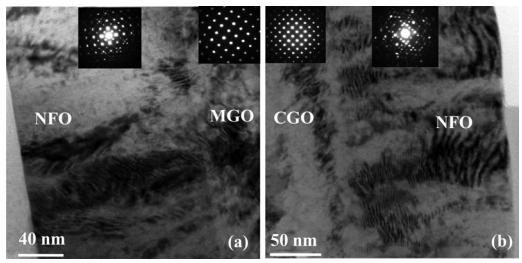

FIG. 2. TEM x-section diffraction contrast image from NFO grown on (a) MGO and (b) CGO substrates. DPs corresponding to substrate and films are superimposed in the figures. DPs have not been rotated to align with the growth direction.

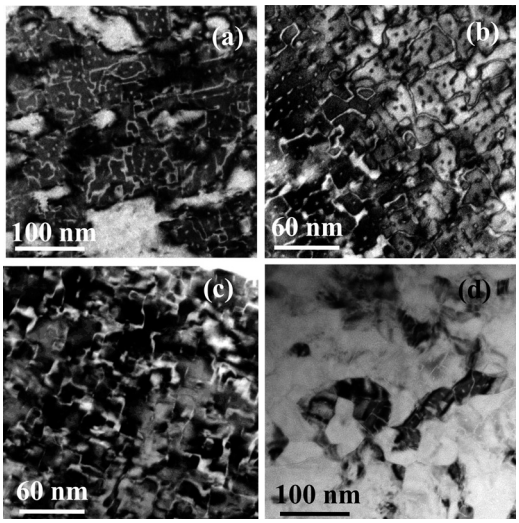

FIG. 3. TEM PV diffraction contrast images from NFO grown on (a) CTO (g=⟨110⟩), (b) MAO (along 001 zone axis), (c) STO (along 001 zone axis), and (d) CGO (g=⟨110⟩), at 550 °C. One can notice reduced APB density in NFO grown on CGO. However, extra spots are present in NFO diffraction pattern grown on CGO and MGO.

Average APB domain size is ~20 nm in case of NFO/MAO. From these observations it is evident that there is a relationship between density of APBs and lattice mismatch.

Further, we have performed aberration corrected high resolution transmission electron microscopy to determine the nature of dark diffuse contrast in NFO film in terms of cation arrangement. One candidate NFO thin film grown on MAO (at 550 °C) is selected for this study. Figure 4(a) shows HRTEM image from dark diffused contrast area. Figure 4(b) shows close up view of atomic arrangement from the same dark diffused area (antiphase domain boundary). The octahedral and tetrahedral atom positions of an ideal spinel structure along ⟨100⟩ are indicated in Fig. 5(a). From NFO film one can image atomic order column by column (along ⟨100⟩, Fig. 5(b)) and this is compared with schematic in Fig. 5(a). Figures 5(c) and 5(d) are schematic and atomic resolution phase contrast images taken from dark contrast area, respectively. In cross section sample geometry, we observe superimposed crystal periodicity from both the domains in projection and Fig. 5(d) is the view of atomic arrangement from a region where two different domains with 1/4 ⟨110⟩ translation vectors are superimposed. In projection all the tetrahedral voids position will appear as filled. From this figure one can visualize that the tetrahedral atom positions have been interchanged between two domains and boundary between domains is responsible for giving rise to the dark diffuse contrast.

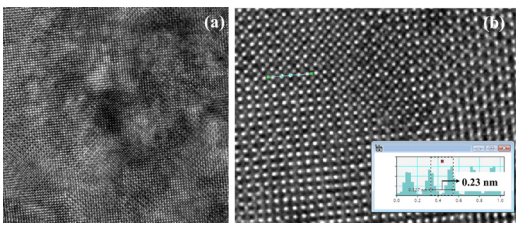

FIG. 4. (Color online) (a) HRTEM image from dark diffused contrast area and magnified view is displayed in (b).

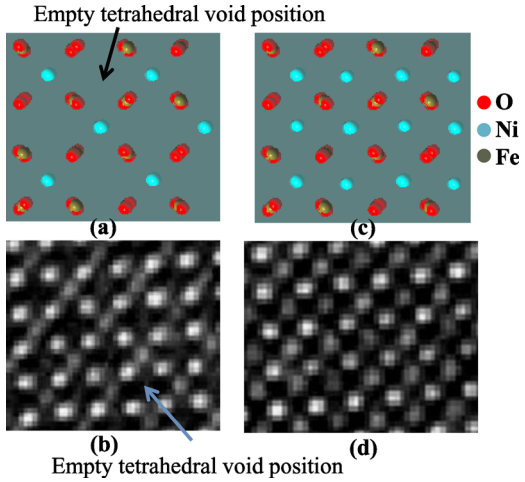

FIG. 5. (Color online) (a) and (b) are the schematic of NFO (considering spinel structure) and corresponding HRTEM image. (c) and (d) are schematic and HRTEM images from two different antiphase domains in projection.

In conclusion, we have compared the formation of APB population in NFO thin film as a function of various substrates. APB formation appears to originate at the film-substrate interface and is observed on all substrates. However, their density appears to decrease with decreasing lattice mismatch on isostructural spinel substrates. Atomic resolution HRTEM images provide direct evidence that cationic arrangement change in the tetrahedral positions in the host oxygen sub lattice as one of the mechanisms responsible for the observation of dark diffuse contrast identified with APBs.

The work at the University of Alabama was supported by ONR under Grant No. N00014-09-1-0119. We thank Professor A. Balbashov of the Moscow Power Engineering Institute for providing the $MgGa_2O_4$, $CoGa_2O_4$, and Co_2TiO_4 substrates.

[1]J. D. Adam, S. V. Krishnaswamy, S. H. Talisa, and K. C. Yoo, J. Magn. Magn. Mater. **83**, 419 (1990).
[2]C. Deng, Y. Zhang, J. Ma, Y. Lin, and C. Nan, J. Appl. Phys. **102**, 074114 (2007).
[3]Y. Zhang, C. Deng, J. Ma, Y. Lin, and C. Nan, Appl. Phys. Lett. **92**, 062911 (2008).
[4]J. J. Yang, Y. G. Zhao, H. F. Tian, L. B. Luo, H. Y. Zhang, Y. J. He, and H. S. Luo, Appl. Phys. Lett. **94**, 212504 (2009).
[5]U. Lüders, A. Barthélemy, M. Bibes, K. Bouzehouane, S. Fusil, E. Jacquet, J.-P. Contour, J.-F. Bobo, J. Fontcuberta, and A. Fert, Adv. Mater. **18**, 1733 (2006).
[6]M. G. Chapline and S. X. Wang, Phys. Rev. B **74**, 014418 (2006).
[7]A. V. Ramos, M.-J. Guittet, J.-B. Moussy, R. Mattana, C. Deranlot, F. Petroff, and C. Gatel, Appl. Phys. Lett. **91**, 122107 (2007).
[8]U. Lüders, M. Bibes, J. F. Bobo, M. Cantoni, R. Bertacco, and J. Fontcuberta, Phys. Rev. B **71**, 134419 (2005).
[9]U. Lüders, G. Herranz, M. Bibes, K. Bouzehouane, E. Jacquet, J.-P. Contour, S. Fusil, J.-F. Bobo, J. Fontcuberta, A. Barthélémy, and A. Fert, J. Appl. Phys. **99**, 08K301 (2006).
[10]J. X. Ma, D. Mazumdar, G. Kim, H. Sato, N. Z. Bao, and A. Gupta, "Robust approach for the growth of epitaxial spinel ferrite films," J. Appl. Phys. (to be published).
[11]M. Luysberg, R. G. S. Sofin, S. K. Arora, and I. V. Shvets, Phys. Rev. B **80**, 024111 (2009).
[12]F. Rigato, S. Estradé, J. Arbiol, F. Peiro, U. Lüders, X. Martí, F. Sánchez, and J. Fontcuberta, Mater. Sci. Eng., B **144**, 43 (2007).
[13]C. L. Jia, M. Lentzen, and K. Urban, Science **299**, 870 (2003).